



Contents lists available at ScienceDirect

## Arabian Journal of Chemistry

journal homepage: [www.ksu.edu.sa](http://www.ksu.edu.sa)Fast fabrication of High-Yield WS<sub>2</sub> nanoscrolls via ultrasound sonication

Thaar M.D. Alharbi

Physics Department, Faculty of Science, Taibah University, Almadinah Almunawarrah 42353, Saudi Arabia

## ARTICLE INFO

## Keywords:

WS<sub>2</sub>  
Nanoscroll  
Probe ultrasonication  
High yield  
Exfoliation

## ABSTRACT

Transforming the bulk of tungsten disulfide (WS<sub>2</sub>) into one-dimensional (1D) nanoscrolls has potential applications in a variety of fields. The current methods for fabricating (1D) WS<sub>2</sub> nanoscrolls suffer from low yields, high temperatures, a complicated fabrication process, and the use of surfactants. We have reported a facile and cost-effective approach for fabricating WS<sub>2</sub> nanoscrolls in high yield using ultrasound probe sonication (20 KHz) from bulk WS<sub>2</sub> in dimethylformamide (DMF) in two hours. Importantly, this simple method achieves a 90 % WS<sub>2</sub> nanoscroll yield. This depends on critical experimental parameters such as the choice of solvent, the initial concentration of WS<sub>2</sub>, and the sonication time. Scanning electron microscopy (SEM) and transmission electron microscopy (TEM) measurements confirm that the nanoscrolls have a closely uniform shape, with an interlayer spacing of ~ 0.62 nm between adjacent layers of WS<sub>2</sub> nanoscrolls. Atomic force microscopy (AFM) reveals that the nanoscrolls have a length of approximately 650 nm and a height profile of 5–10 nm, indicating their formation from multiple layers of WS<sub>2</sub>. We further investigate the fabricated nanoscrolls using other techniques such as X-ray photoelectron spectroscopy (XPS), X-ray diffraction (XRD), and Raman spectroscopy.

## 1. Introduction

In recent years, intense interest has been paid to the layered two-dimensional (2D) transition metal dichalcogenides (TMDs). 2D atomically thin nanosheets of transition metal dichalcogenides (TMDs) have attracted attention as one of the most promising materials for various applications owing to their low cost, easy preparation, large surface areas, and unique chemical and physical properties (Manzeli et al., 2017; Han et al., 2018).

Converting two-dimensional (2D) nanosheets into one-dimensional (1D) nanoscrolls is an interesting method of fabricating new nanomaterials (Li et al., 2017; Han et al., 2018; Lv et al., 2015; Dong et al., 2021). The tubular structures of nanoscrolls are different from 2D thin nanosheets and exhibit outstanding physical and chemical properties, as predicted in many theoretical studies (Sharifi et al., 2013; Lai et al., 2016; Wang et al., 2020). Transforming 2D tungsten disulfide (WS<sub>2</sub>) nanosheets into 1D WS<sub>2</sub> nanoscrolls by rolling opens the door for 1D tubular-structured materials with unique properties (Aftab, Iqbal, and Rim, 2023), such as superior electronic and electromechanical properties. These WS<sub>2</sub> nanoscrolls can be used in many applications including tribology, field-effect transistors, catalysis, and energy storage (Li et al., 2017; Han et al., 2018; Lv et al., 2015; Dong et al., 2021).

TMDs nanoscrolls have been fabricated using different chemical and physical strategies, including strain-induced scrolling (Zhou et al., 2019; Hao, Yang, and Gao, 2016), supercritical fluids (Thangasamy and Sathish, 2016), amphiphilic organic molecules (Choi and Suh, 2018), argon

plasma (Meng et al., 2016), alkaline droplets (Wang et al., 2020), vortex fluidic device (VFD) (Alharbi et al., 2022; Alharbi et al., 2018), and organic solvents (Fang et al., 2018; Cui et al., 2018; Deng et al., 2019). Among the fabrication methods, chemical vapor deposition (CVD) has been widely used to synthesize atomically flat WS<sub>2</sub> nanosheets, following which a few drops of an organic solvent are added to the flat WS<sub>2</sub> sheets, making them fold to form the structure of a nanoscroll (Fang et al., 2018; Wang et al., 2020). Zhao et al. successfully fabricated WS<sub>2</sub> nanoscrolls with a length of 10 μm using CVD-grown monolayer WS<sub>2</sub> nanosheets (Zhao et al., 2022). Ethanol, as an organic solvent, was dropped on the WS<sub>2</sub> flat nanosheets, and during ethanol evaporation, the WS<sub>2</sub> nanosheet edge rolled up to form the scroll structure (Fang et al., 2018).

Another approach for fabricating nanoscrolls structure is sonication. Sonication is a simple and fast technique and has been widely used to fabricate nanoscrolls under ambient conditions because of its advantages such as low cost and mass production. Pradeep et al. used an ultrasonicator for the fabrication of graphene nanoscrolls in a mixture of ethanol and water (Pradeep et al., 2021). Additionally, Purkait et al. successfully fabricated graphene oxide nanoscrolls with tunable dimensions via low-frequency sonication (20 KHz) (Sontakke and Purkait, 2020). However, these approaches have some limitations, for example, some methods require high temperature, complex steps or use surfactants and harsh chemicals that can potentially damage the properties of the fabricated material and generate a waste stream. Therefore, a low-cost and simple technique for fabricating WS<sub>2</sub> nanoscrolls is required.

<https://doi.org/10.1016/j.arabjc.2024.105819>

Received 19 January 2024; Accepted 30 April 2024

Available online 1 May 2024

1878-5352/© 2024 The Author. Published by Elsevier B.V. on behalf of King Saud University. This is an open access article under the CC BY-NC-ND license (<http://creativecommons.org/licenses/by-nc-nd/4.0/>).

To the best of our knowledge, there have been no previous attempts to directly scrolling WS<sub>2</sub> from bulk WS<sub>2</sub> in high yield using an ultrasonicator in dimethylformamide (DMF). This study reports the fabrication of WS<sub>2</sub> nanoscrolls from bulk WS<sub>2</sub> using DMF only, thereby avoiding the use of harsh chemicals and surfactants. WS<sub>2</sub> nanoscrolls were successfully fabricated via probe ultrasonication at room temperature using a single solvent, namely, DMF. The fabricated WS<sub>2</sub> nanoscrolls were characterized using different techniques including SEM, AFM, TEM, STEM, XRD, Raman and XPS.

## 2. Experimental section

### 2.1. Chemicals and materials

A WS<sub>2</sub> powder with a lateral dimension size in the range of 2 μm was purchased from Sigma-Aldrich. Ultrapure water (18.2 MΩ cm; Milli-Q Direct 8) was used in all experiments. DMF (purity = 99 %) was purchased from Sigma-Aldrich, and toluene (purity = 99 %) was purchased from Alfa Aesar.

### 2.2. Materials fabrication

The fabrication of WS<sub>2</sub> nanoscrolls from bulk WS<sub>2</sub>: Bulk WS<sub>2</sub> with a lateral dimension size of ~ 2 μm was dispersed in DMF. Briefly, 300 mg of the WS<sub>2</sub> powder was added to 60 mL of DMF in a 100-mL beaker and sonicated using a bath sonicator for 15 min to make a colloid suspension. No change in the WS<sub>2</sub> structure was observed at this stage. Then, the WS<sub>2</sub> solution was sonicated using the probe ultrasonicator (ultrasonic processor SONIC Vibra cell with a probe Model 18) for 2 h (2 h) at a low frequency of 20 KHz. The solution was placed in an ice bath to ensure its temperature remained close to room temperature (<30 °C). After 2 h, the product comprising high quantities of WS<sub>2</sub> nanoscrolls was collected. The yield of WS<sub>2</sub> nanoscrolls was 90 %, which is calculated using the volume and concentration of the bulk WS<sub>2</sub> (5 mg/mL) and the quantity of the isolated and dried nanoscrolls of WS<sub>2</sub>, the processed solution of WS<sub>2</sub> nanoscrolls was centrifuged at 9980 g for 10 min to remove unscrolled sheets. About 90 % of the top supernatant was then collected by micropipette and from this the yield was estimated to be 90 %.

### 2.3. Characterization

WS<sub>2</sub> nanoscrolls were characterized using scanning electron microscopy (SEM; FEI Quanta 450 high-resolution field-emission scanning electron microscope; voltage = 10 kV). The morphology of WS<sub>2</sub> nanoscrolls was characterized using atomic force microscopy (AFM; Nanoscope 8.10; tapping mode) and transmission electron microscopy (TEM; TECNAI 20 microscope, operating at 120 and 200 kV). Scanning TEM (STEM) analysis and compositional mapping were performed using an aberration-corrected FEI Titan Themis transmission electron microscope operating at 200 kV equipped with an energy-dispersive X-ray detector. The chemical composition of the WS<sub>2</sub> nanoscrolls was also studied via X-ray photoelectron spectroscopy (XPS), and a hemispherical analyzer (SPECS) was performed using an X-ray source with Mg Kα line (hν = 1253.6 eV) with a base pressure of a few 10<sup>-10</sup> mbar. X-ray powder diffraction (XRD) data were collected using a Bruker Advanced D8 diffractometer (capillary stage) using Cu Kα radiation (λ = 1.5418 Å, 50 kW/40 mA, 2θ = 10–80°). Raman measurements were recorded at an excitation wavelength of 532 nm (≤5mW) at room temperature.

## 3. Results and discussion

### 3.1. Fabrication of WS<sub>2</sub> nanoscrolls

In this contribution, we have reported a simple, straightforward, and scalable method for directly scrolling WS<sub>2</sub> from their bulk in DMF,

which is cost-effective and can be achievable in most laboratories. The procedure for fabricating WS<sub>2</sub> nanoscrolls from their bulk material via ultrasonication is illustrated schematically in Fig. 1a. The scanning electron microscopy (SEM) image of bulk WS<sub>2</sub> powder revealed the typical multilayered structure with a lateral size ranging from sub micrometer to a few micrometers (Fig. 1b). A dramatic change can be seen in the morphology of the bulk WS<sub>2</sub> after ultrasonication processing with the nanoscroll formation (Fig. 1c), depending on the time processing, solvent choice, and concentration of the bulk WS<sub>2</sub>.

Initially, we dispersed the bulk WS<sub>2</sub> powder in various solvents, such as N-methyl-2-pyrrolidone (NMP), water, and ethanol. Despite these solvent systems being reported in the literature for exfoliating TMD, some of them were forming scroll structures either in a low yield or requiring complex steps to fabricate such structures. (Cui et al., 2018; Thangasamy and Sathish, 2016; Suh, 2016) They were ineffective in the probe ultrasonication processing with a concentration of 5 mg/mL for two hours and at a 20 KHz frequency (Figs. S1–S3).

Next, we chose DMF as the solvent, which led to the formation of WS<sub>2</sub> nanoscrolls in a high yield of approximately 90 %, as we will discuss below. The effects of other parameters, including the concentration of WS<sub>2</sub> (i.e., 3, 5 and 10 mg/mL; Fig. S4 and S5c) and sonication time (i.e., 30 mins, 1 h, and 2 h) on WS<sub>2</sub> nanoscroll formation were studied (Fig. S5).

Establishing the optimal conditions for fabricating WS<sub>2</sub> nanoscrolls using DMF as a solvent at a concentration of 5 mg/mL, the black suspension of the bulk WS<sub>2</sub> powder was sonicated in a bath sonicator for 15 min and then placed in a 100-mL glass beaker. The probe ultrasonicator was placed in the middle of the solution from the top and set on a low frequency of 20 KHz from 2 h (Fig. 1b). The morphology of WS<sub>2</sub> changes dramatically from flat flakes to WS<sub>2</sub> nanoscrolls after the probe ultrasonication (20 KHz) (Fig. 1c).

### 3.2. Characterization of WS<sub>2</sub> nanoscrolls

The structure and morphology of the fabricated WS<sub>2</sub> nanoscrolls were systematically investigated by SEM, AFM, TEM, HRTEM, STEM, XRD, Raman, and XPS. Fig. 2a, b shows low-magnification SEM images of the bulk WS<sub>2</sub> before processing; they exhibit an irregular structure and sizes ranging from a few micrometers to tens of micrometers. After processing the bulk power of WS<sub>2</sub> using the probe ultrasonication under the optimized conditions; including “concentration, low frequency, solvent and reaction time”. They have dramatically changed from the 2D bulk WS<sub>2</sub> structure and completely converted to 1D nanoscrolls of WS<sub>2</sub>, as it can be clearly observed from SEM images in Fig. 2c–f. In addition, no bulk structure from WS<sub>2</sub> flakes is seen in the solution after processing (Fig. 2c–f).

AFM measurements were performed to characterize the structure of WS<sub>2</sub> nanoscrolls and investigate their size and shape (Fig. 3), AFM images further confirm that the fabricated WS<sub>2</sub> nanoscrolls exhibit a nanoscroll structure with a closely uniform shape (Fig. 3a–d). They have a length distribution of 650 nm (Fig. 3e), which is consistent with what is observed by SEM. The height profile of the selected WS<sub>2</sub> nanoscrolls revealed a height ranging between 5 and 10 nm, (Fig. 3f), indicating that more than one layer of WS<sub>2</sub> was rolled up during the processing, which is in good agreement with the literature (Thangasamy, Raj, and Sathish, 2020).

The nanoscrolls of WS<sub>2</sub> were further investigated using TEM and HRTEM. Fig. 4a, b shows a low and high magnification TEM image of the WS<sub>2</sub> nanoscrolls, which unambiguously confirms the formation of WS<sub>2</sub> nanoscrolls. The HRTEM image, Fig. 4c, shows that in the nanoscrolls formed using multiple layers of WS<sub>2</sub>, the interlayer spacing between adjacent layers of WS<sub>2</sub> nanoscrolls is ~ 0.62 nm (Fang et al., 2018; Cui et al., 2018). Additionally, we performed the elemental mapping of WS<sub>2</sub> nanoscrolls using high-resolution STEM. The high-angle annular dark-field (HAADF) STEM image shows that the WS<sub>2</sub> nanoscrolls have a tubular structure. The elemental mapping shows the presence of W and S

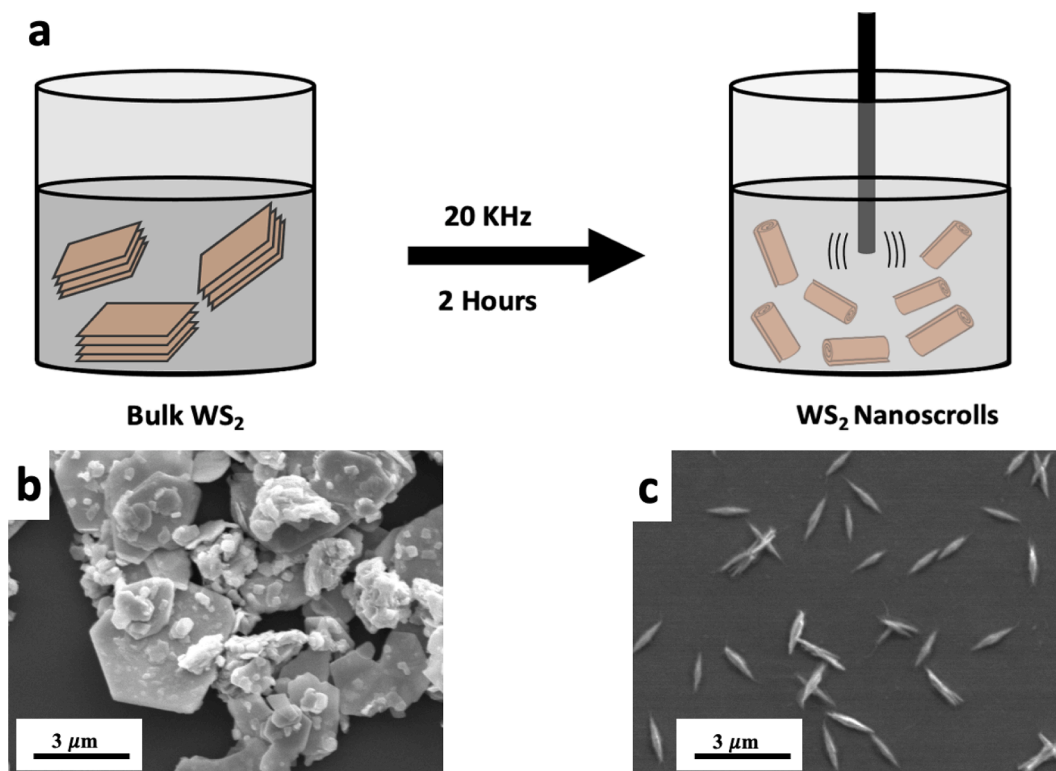


Fig. 1. (a) Schematic of the experimental procedure for fabricating WS<sub>2</sub> nanoscrolls via probe ultrasonication in DMF with a concentration of 5 mg/mL. SEM image of (b) bulk WS<sub>2</sub> and (c) WS<sub>2</sub> nanoscrolls.

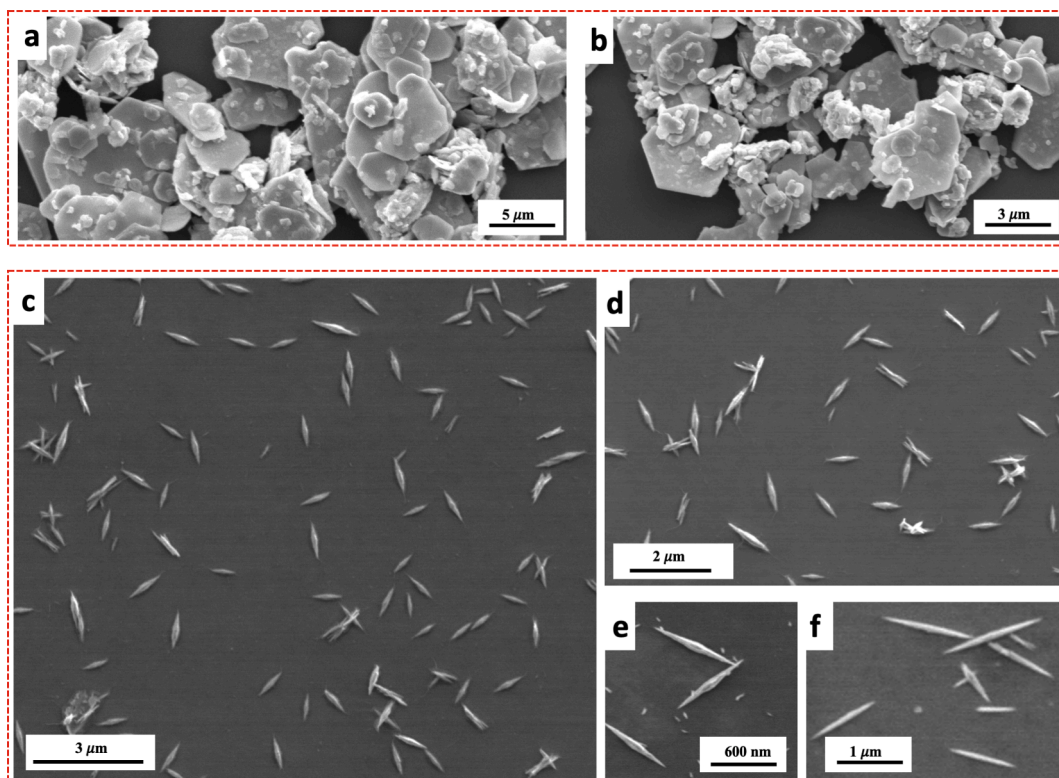


Fig. 2. SEM images of (a-b) bulk WS<sub>2</sub> (before processing) and (c-f) WS<sub>2</sub> nanoscrolls (after processing using the probe ultrasonication under the optimized conditions).

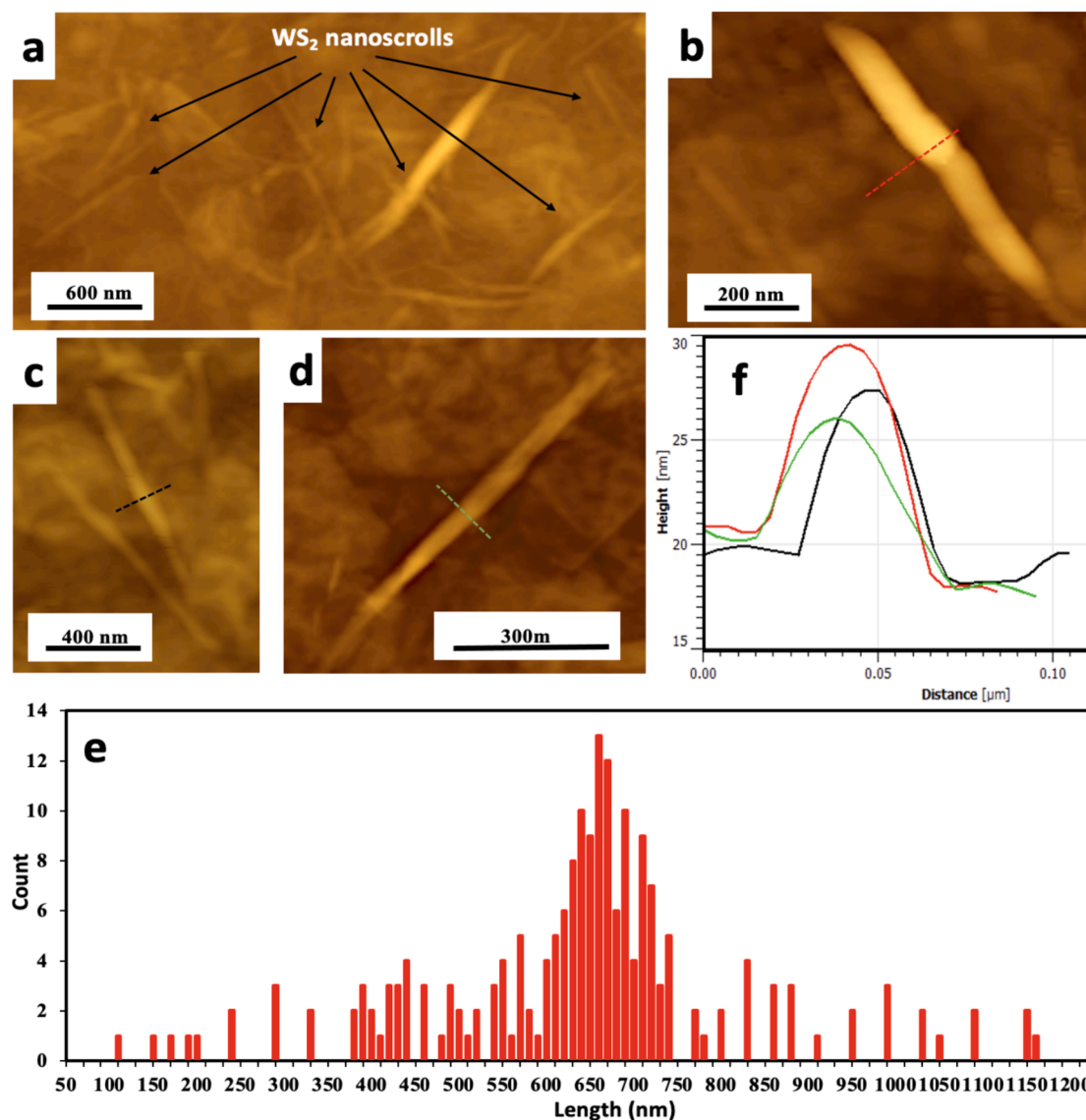


Fig. 3. (a-d) AFM images, (e) The length distribution and (f) The height profiles of WS<sub>2</sub> nanoscrolls.

throughout the WS<sub>2</sub> nanoscrolls (Fig. 4d–f). These findings are in line with the above SEM and AFM results.

To further investigate the structure of WS<sub>2</sub> nanoscrolls, X-ray diffraction (XRD) was conducted for both the bulk and nanoscrolls of WS<sub>2</sub>. For the bulk WS<sub>2</sub>, (Fig. 5a), there are five obvious and sharp diffraction peaks at 17°, 35°, 40°, 53° and 72°, which can be assigned to the (002), (004), (100), (103) and (105) planes, which reflects of the hexagonal crystal structure of 2H-WS<sub>2</sub>. (Stengl and Henych, 2013) After fabricating of WS<sub>2</sub> nanoscrolls, (Fig. 5b) only one main diffraction peak at 2θ of 14.97° corresponding to the crystal plane of (002). The two weak peaks at 2θ = 35° and 53° in the XRD pattern of the WS<sub>2</sub> nanoscrolls are attributed to the (004) and (103) diffractions, respectively (Thangasamy, Raj, and Sathish, 2020; Thangasamy and Sathish, 2016). Sathish et al. also reported the appearance of similar diffraction peaks after forming WS<sub>2</sub> nanoscrolls using energy efficient supercritical fluid processing at 400°C (Thangasamy, Raj, and Sathish, 2020).

Raman spectroscopy is employed to characterize the crystal structure of the bulk WS<sub>2</sub> and nanoscrolls, using 532 nm excitation as shown in Fig. 5c, d. There are two characteristic peaks can be observed for both materials, assignable to the (E<sub>2g</sub>) mode at 350 cm<sup>-1</sup> and the (A<sub>1g</sub>) mode at 420 cm<sup>-1</sup>, (Fig. 5c), corresponding to the in-plane W – S vibrations and sulfur out-of-plane vibrations (Adilbekova et al., 2020; Liu and

Komatsu, 2016), respectively, which indicates the fabricated WS<sub>2</sub> nanoscrolls show a good crystallinity. (Adilbekova et al., 2020; Liu and Komatsu, 2016) After fabricating nanoscroll structure from the bulk WS<sub>2</sub>, (Fig. 5d), the (E<sub>2g</sub>) mode peak has a red shift, from 350 to 348 cm<sup>-1</sup> compared with those of the starting WS<sub>2</sub>, which can be attributed to the bond strain present in the WS<sub>2</sub> nanoscrolls after processing (Yue et al., 2020; Wang et al., 2020). Whereas there is a blue-shifted for (A<sub>1g</sub>) mode of the WS<sub>2</sub> nanoscrolls from 420 to 418.3 cm<sup>-1</sup>, which can be attributed to the van der Waals interactions between neighboring layers in the nanoscrolls structure (Aftab, Iqbal, and Rim, 2023; Wang et al., 2016).

XPS was used to study the elemental composition of bulk WS<sub>2</sub> and WS<sub>2</sub> nanoscrolls. Herein, the expected elements in the XPS spectra are W and S. Fig. 6 shows the high-resolution XPS spectra of bulk and nanoscrolls of WS<sub>2</sub>. In the XPS spectrum of bulk WS<sub>2</sub>, two strong peaks are observed at 33.14 and 35.45 eV, which correspond to W 4f<sub>7/2</sub> and W 4f<sub>5/2</sub>, respectively (Fig. 6a) (Ghosh et al., 2022; Nethravathi et al., 2013). Similarly, the S 2p XPS spectra of bulk WS<sub>2</sub> show two peaks at 162.75 and 163.93 eV, corresponding to S 2p<sub>3/2</sub> and S 2p<sub>1/2</sub>, respectively (Mao et al., 2013; Nethravathi et al., 2013) (Fig. 6b). After the formation of WS<sub>2</sub> nanoscrolls, two additional main peaks can be observed at 37.10 and 39.25 eV in the W 4f XPS spectrum of WS<sub>2</sub> nanoscrolls, which are assigned to W–O. These peaks may appear in the XPS spectra because



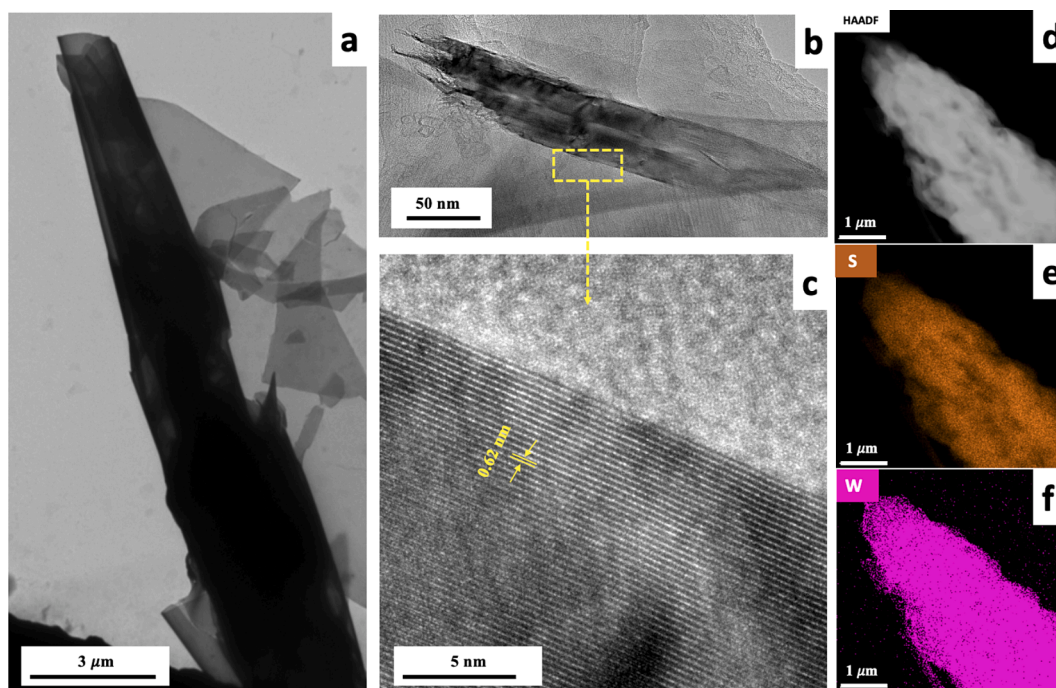


Fig. 4. (a-b) TEM images, (c) HRTEM image, (d) STEM image, and (e-f) elemental mappings of WS<sub>2</sub> nanoscrolls.

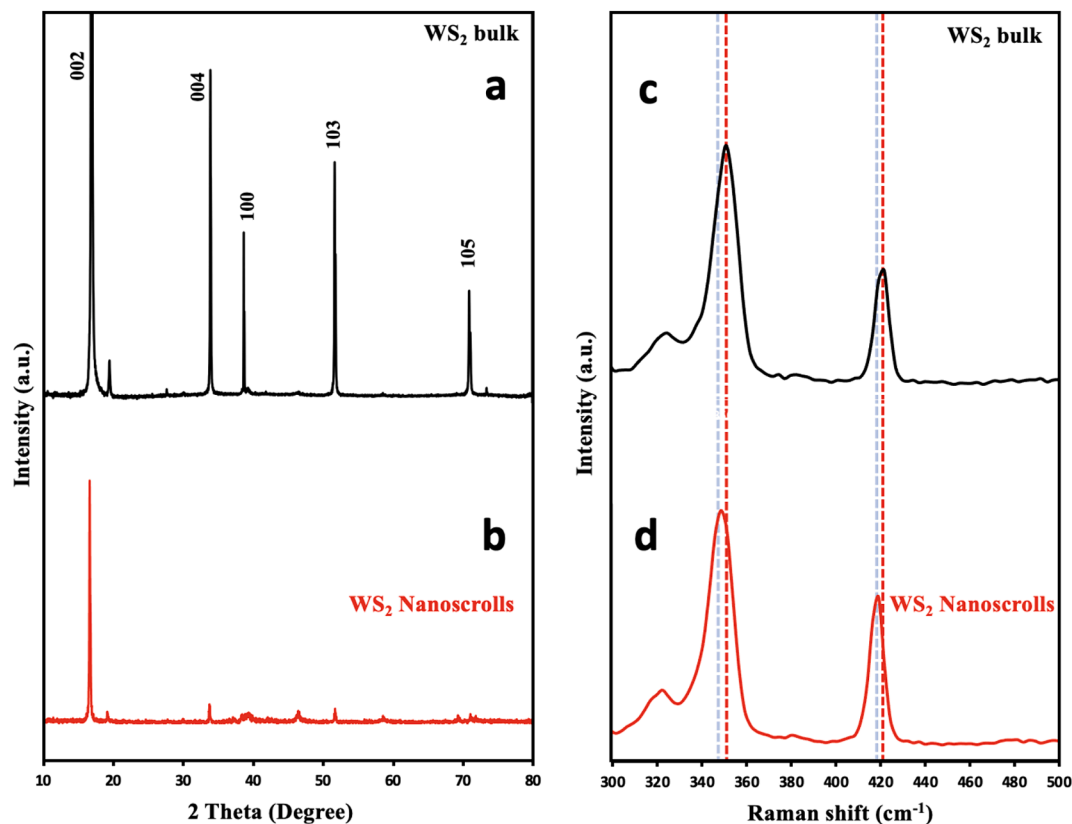


Fig. 5. XRD patterns of (a) bulk WS<sub>2</sub> and (b) WS<sub>2</sub> nanoscrolls and Raman spectra of (c) bulk WS<sub>2</sub> and (d) WS<sub>2</sub> nanoscrolls.

after processing, the fabricated nanoscrolls are oxidized (Fig. 6c) (Huang et al., 2018; Zhou et al., 2014; Cohen et al., 2023). Similarly, the S 2p XPS spectra of the WS<sub>2</sub> nanoscrolls show another main peak at 169.7 eV, which is attributed to S<sup>6+</sup> from oxidized S (Fig. 6d) (Miao et al., 2022).

### 3.3. Mechanism of WS<sub>2</sub> nanoscroll formation

The schematic of the mechanism for the formation of WS<sub>2</sub> nanoscrolls is shown in Fig. 7. The experiment was performed using the probe ultrasonication at a low frequency (20 KHz) because high-frequency

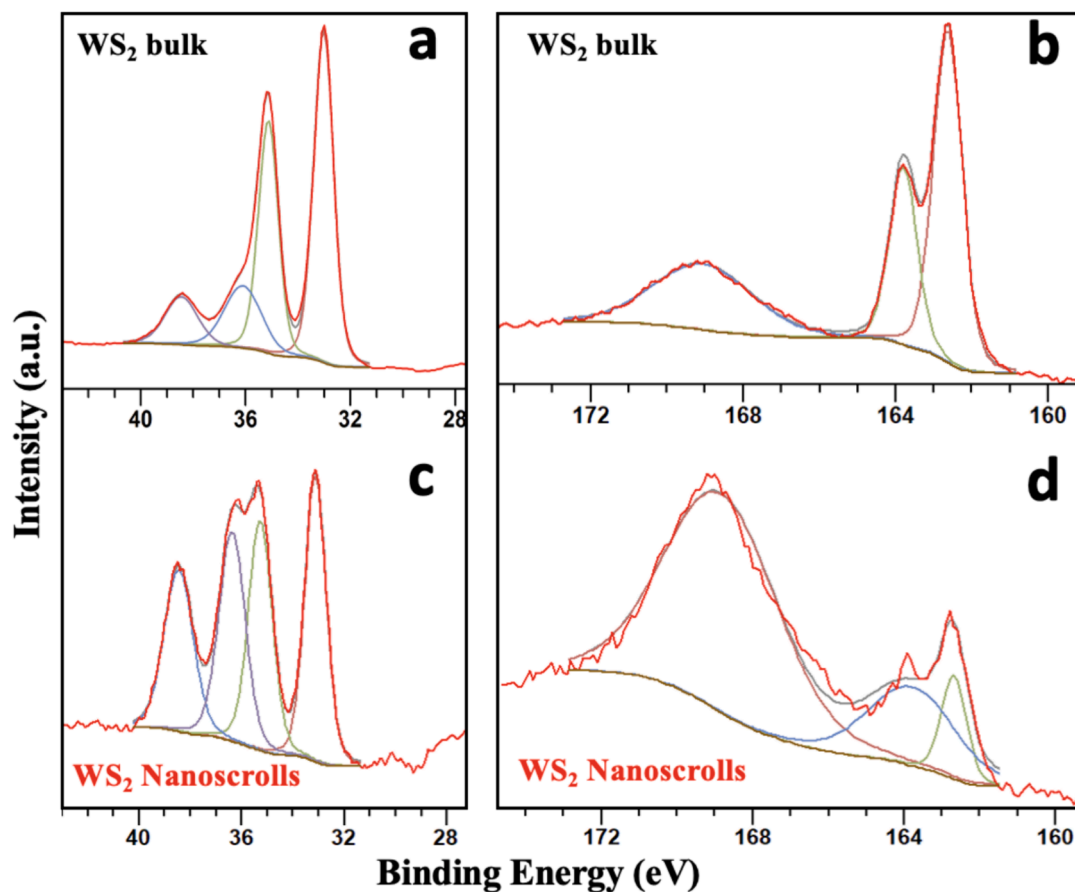


Fig. 6. High-resolution W 4f and S 2p XPS spectra of bulk  $WS_2$  (a-b) and  $WS_2$  nanoscrolls (c-d).

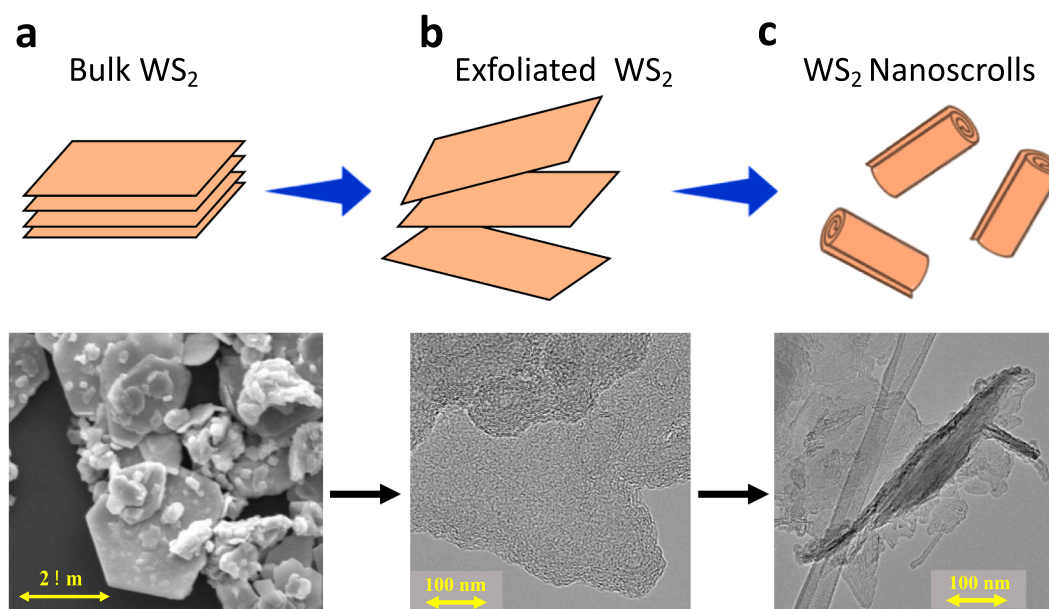


Fig. 7. Schematic showing the mechanism for the formation of  $WS_2$  nanoscrolls.

ultrasonic waves can change and may damage the crystal structure of the  $WS_2$  materials and destroy their properties (Fig. S6). (Gopalakrishnan, Damien, and Shaijumon, 2014) The mechanism of  $WS_2$  nanoscroll formation from bulk  $WS_2$  is as follows: First, the bulk  $WS_2$  is exfoliated by the force induced by cavitation bubble collapse. (Telkhozhayeva et al., 2021; Deshmukh et al., 2019) When the cavitation-

induced bubbles collapse with massive energy, and shock stress waves will act on the bulk  $WS_2$  crystal rapidly (Fig. 7a), resulting in breaking down bulk  $WS_2$  into smaller flakes in the solution as well as exfoliating  $WS_2$  into nanosheets of  $WS_2$  and that occurred after 1 h of sonication, as shown in Fig. 7b, the formation of nanosheets is well understood, as reported by several researchers. (Telkhozhayeva et al., 2021; Deshmukh

et al., 2019) Increasing the probe ultrasonication time to 2 h resulted in the scrolling of these exfoliated WS<sub>2</sub> nanosheets and the formation of the 1D structure of WS<sub>2</sub> nanoscrolls (Fig. 7c).

#### 4. Conclusion

In summary, we have successfully fabricated WS<sub>2</sub> nanoscrolls in high yield (90 %) directly from their bulk WS<sub>2</sub> in DMF using ultrasonication (20 KHz) for two hours. This simple, low-cost, and scalable method eliminates the need for surfactant or other harsh chemicals and can be achieved in any laboratory. Crucial parameters such as choice of solvent, WS<sub>2</sub> concentration, and sonication time are systematically explored to establish the optimal conditions for fabricating WS<sub>2</sub> nanoscrolls in high yields. SEM and TEM characterizations confirmed the successful fabrication of WS<sub>2</sub> nanoscrolls with a closely uniform shape. AFM measurements showed that the 1D WS<sub>2</sub> nanoscrolls have a height of 5–10 nm with a length distribution centered at 650 nm. This developed strategy for fabricating WS<sub>2</sub> nanoscrolls on demand, with the ability to prepare them in high yield, paves the way for developing WS<sub>2</sub> nanoscroll applications.

#### Disclosure statement

The author has no conflict of interest to declare.

#### CRediT authorship contribution statement

**Thaar M.D. Alharbi:** Formal analysis, Investigation, Methodology, Supervision, Visualization, Writing – original draft, Writing – review & editing.

#### Declaration of Competing Interest

The authors declare that they have no known competing financial interests or personal relationships that could have appeared to influence the work reported in this paper.

#### Acknowledgement

Thaar Alharbi thanks Prof. Colin L. Raston from Flinders University, Adelaide, Australia for his help and support. The authors extend their appreciation to the Deputyship for Research & Innovation, Ministry of Education in Saudi Arabia for funding this work through Research Supporting Project number (445-9-766).

#### Appendix A. Supplementary data

Supplementary data to this article can be found online at <https://doi.org/10.1016/j.arabjc.2024.105819>.

#### References

- Adilbekova, B., Lin, Y., Yengel, E., Faber, H., Harrison, G., Firdaus, Y., El-Labban, A., Anjum, D.H., Tung, V., Anthopoulos, T.D., 2020. Liquid phase exfoliation of MoS<sub>2</sub> and WS<sub>2</sub> in aqueous ammonia and their application in highly efficient organic solar cells. *J. Mater. Chem. C* 8, 5259–5264.
- Aftab, S., Iqbal, M.Z., Rim, Y.S., 2023. Recent Advances in Rolling 2D TMDs Nanosheets into 1D TMDs Nanotubes/Nanoscrolls. *Small* 19, 2205418.
- Alharbi, T.M.D., Elmas, S., Alotabi, A.S., Andersson, M.R., Raston, C.L., 2022. Continuous Flow Fabrication of MoS<sub>2</sub> Scrolls for Electrocatalytic Hydrogen Evolution. *ACS Sustain. Chem. Eng.*
- Alharbi, Thaar MD, David Harvey, Ibrahim K Alsulami, Nazila Dehbari, Xiaofei Duan, Robert N Lamb, Warren D Lawrence, and Colin L Raston. 2018. 'Shear stress mediated scrolling of graphene oxide', Carbon.
- Choi, K.H., Suh, D.H., 2018. A vacancy-driven phase transition in MoX<sub>2</sub> (X: S, Se and Te) nanoscrolls. *Nanoscale* 10, 7918–7926.
- Cohen, A., Mohapatra, P.K., Hettler, S., Avinash Patsha, K.V.L.V., Narayanachari, P.S., Cavin, J., Rondinelli, J.M., Bedzyk, M., Dieguez, O., 2023. Tungsten Oxide Mediated Quasi-van der Waals Epitaxy of WS<sub>2</sub> on Sapphire. *ACS Nano* 17, 5399–5411.
- Cui, X., Kong, Z., Gao, E., Huang, D., Hao, Y., Shen, H., Di, C.-a., Zhiping, Xu., Zheng, J., Zhu, D., 2018. Rolling up transition metal dichalcogenide nanoscrolls via one drop of ethanol. *Nat. Commun.* 9, 1–7.
- Deng, W., You, C., Chen, X., Wang, Y.I., Li, Y., Feng, B., Shi, K.e., Chen, Y., Sun, L., Zhang, Y., 2019. High-Performance Photodiode Based on Atomically Thin WSe<sub>2</sub>/MoS<sub>2</sub> Nanoscroll Integration. *Small* 15, 1901544.
- Deshmukh, A.R., Jeong, J.W., Lee, S.J., Park, G.U., Kim, B.S., 2019. Ultrasound-assisted facile green synthesis of hexagonal boron nitride nanosheets and their applications. *ACS Sustain. Chem. Eng.* 7, 17114–17125.
- Dong, J., Zhang, L., Bin, Wu., Ding, F., Liu, Y., 2021. Theoretical Study of Chemical Vapor Deposition Synthesis of Graphene and Beyond: Challenges and Perspectives. *The Journal of Physical Chemistry Letters* 12, 7942–7963.
- Fang, Xiangru, Pei Wei, Lin Wang, Xiaoshan Wang, Bo Chen, Qiyuan He, Qiuyan Yue, Jindong Zhang, Weihao Zhao, Jialiang %J ACS applied materials Wang, and interfaces. 2018. 'Transforming Monolayer Transition-Metal Dichalcogenide Nanosheets into One-Dimensional Nanoscrolls with High Photosensitivity', 10: 13011-18.
- Ghosh, R., Singh, M., Chang, L.W., Hung-I Lin, Yu., Chen, S., Muthu, J., Papnai, B., Kang, Y.S., Liao, Y.-M., Bera, K.P., 2022. Enhancing the Photoelectrochemical Hydrogen Evolution Reaction through Nanoscrolling of Two-Dimensional Material Heterojunctions. *ACS Nano* 16, 5743–5751.
- Gopalakrishnan, D., Damien, D., Shaijumon, M.M., 2014. MoS<sub>2</sub> quantum dot-interspersed exfoliated MoS<sub>2</sub> nanosheets. *ACS Nano* 8, 5297–5303.
- Han, G.H., Duong, D.L., Keum, D.H., Yun, S.J., Lee, Y.H., 2018. van der Waals metallic transition metal dichalcogenides. *Chem. Rev.* 118, 6297–6336.
- Hao, S., Yang, B., Gao, Y., 2016. 'fracture-Induced Nanoscrolls from CVD-Grown Monolayer Molybdenum Disulfide', *Physica Status Solidi (RRL)–Rapid Research Letters* 10, 549–553.
- Huang, L., Yang, J., Zhou, W., Liu, K., Zhu, D., Chen, Y., 2018. Nanoscale tungsten nitride/nitrogen-doped carbon as an efficient non-noble metal catalyst for hydrogen and oxygen recombination at room temperature in nickel-iron batteries. *RSC Adv.* 8, 35343–133537.
- Lai, Z., Chen, Y.e., Tan, C., Zhang, X., Zhang, H.a., 2016. Self-assembly of two-dimensional nanosheets into one-dimensional nanostructures. *Chem* 1, 59–77.
- Li, H., Li, Y., Aljarb, A., Shi, Y., Li, L.-J., 2017. Epitaxial growth of two-dimensional layered transition-metal dichalcogenides: growth mechanism, controllability, and scalability. *Chem. Rev.* 118, 6134–6150.
- Liu, G., Komatsu, N., 2016. Readily available "stock solid" of MoS<sub>2</sub> and WS<sub>2</sub> nanosheets through solid-phase exfoliation for highly concentrated dispersions in water. *ChemNanoMat* 2, 500–553.
- Lv, R., Robinson, J.A., Schaak, R.E., Sun, Du., Sun, Y., Mallouk, T.E., Terrones, M., 2015. Transition metal dichalcogenides and beyond: synthesis, properties, and applications of single- and few-layer nanosheets. *Acc. Chem. Res.* 48, 56–64.
- Manzeli, S., Ovchinnikov, D., Pasquier, D., Yazyev, O.V., Kis, A., 2017. 2D transition metal dichalcogenides. *Nat. Rev. Mater.* 2, 1–15.
- Mao, X., Yan, Xu., Xue, Q., Wang, W., Gao, D., 2013. Ferromagnetism in exfoliated tungsten disulfide nanosheets. *Nanoscale Res. Lett.* 8, 1–6.
- Meng, J., Wang, G., Li, X., Xiaobo, Lu., Zhang, J., Hua, Yu., Chen, W., Luojun, Du., Liao, M., Zhao, J., 2016. Rolling up a monolayer MoS<sub>2</sub> sheet. *Small* 12, 3770–13374.
- Miao, W., Gai, X., Zhao, F., Wang, J., 2022. Excitation induced asymmetric fluorescence emission in 2D-WS<sub>2</sub> quantum dots. *Materials Advances* 3, 1172–11179.
- Nethravathi, C., Anto Jeffery, A., Rajamathi, M., Kawamoto, N., Tenne, R., Golberg, D., Bando, Y., 2013. Chemical unzipping of WS<sub>2</sub> nanotubes. *ACS Nano* 7, 7311–7737.
- Pradeep, N., Upendra Raju, A., Venkataraman, U., 2021. Influence of probe amplitude on the preparation of graphene scroll by probe ultrasonicator technique. *Mater. Today: Proc.* 45, 4012–4409.
- Sharifi, Tiva, Eduardo Gracia-Espino, Hamid Reza Barzegar, Xueen Jia, Florian Nitze, Guangzhi Hu, Per Nordblad, Cheuk-Wai Tai, and Thomas Wågberg. 2013. 'Formation of nitrogen-doped graphene nanoscrolls by adsorption of magnetic γ-Fe<sub>2</sub>O<sub>3</sub> nanoparticles', *Nature communications*, 4: ncomms3319.
- Sontakke, A.D., Purkait, M.K., 2020. Fabrication of ultrasound-mediated tunable graphene oxide nanoscrolls. *Ultrason. Sonochem.* 63, 104976.
- Stengl, V., Henych, J., 2013. Strongly luminescent monolayered MoS<sub>2</sub> prepared by effective ultrasound exfoliation. *Nanoscale* 5, 3387–3394.
- Suh, D.H., 2016. Evolution of a high local strain in rolling up MoS<sub>2</sub> sheets decorated with Ag and Au nanoparticles for surface-enhanced Raman scattering. *Nanotechnology* 28, 025603.
- Telkhozhayeva, M., Teblum, E., Konar, R., Girshevitz, O., Perelshtein, I., Aviv, H., Tischler, Y.R., Nessim, G.D., 2021. Higher ultrasonic frequency liquid phase exfoliation leads to larger and monolayer to few-layer flakes of 2D layered materials. *Langmuir* 37, 4504–4514.
- Thangasamy, P., Raj, J.A., Sathish, M., 2020. Transformation of multilayer WS<sub>2</sub> nanosheets to 1D luminescent WS<sub>2</sub> nanostructures by one-pot supercritical fluid processing for hydrogen evolution reaction. *Mater. Sci. Semicond. Process.* 119, 105167.
- Thangasamy, P., Sathish, M., 2016. Rapid, one-pot synthesis of luminescent MoS<sub>2</sub> nanoscrolls using supercritical fluid processing. *J. Mater. Chem. C* 4, 1165–2119.
- Wang, F., Kinloch, I.A., Wolferson, D., Tenne, R., Zak, A., O'Connell, E., Bangert, U., Young, R.J., 2016. Strain-induced phonon shifts in tungsten disulfide nanoplatelets and nanotubes. *2D Materials* 4, 015007.
- Wang, L., Yue, Q., Pei, C., Fan, H., Dai, J., Huang, X., Li, H., Huang, W., 2020. Scrolling bilayer WS<sub>2</sub>/MoS<sub>2</sub> heterostructures for high-performance photo-detection. *Nano Res.* 13, 959–966.
- Yue, Q., Wang, L., Fan, H., Zhao, Y., Wei, C., Pei, C., Song, Q., Huang, X., Li, H., 2020. Wrapping plasmonic silver nanoparticles inside one-dimensional nanoscrolls of

- transition-metal dichalcogenides for enhanced photoresponse. *Inorg. Chem.* 60, 4226–4235.
- Zhao, Y., You, H., Li, X., Pei, C., Huang, X., Li, H., 2022. Solvent-Free Preparation of Closely Packed MoS<sub>2</sub> Nanoscrolls for Improved Photosensitivity. *ACS Appl. Mater. Interfaces* 14, 9515–9524.
- Zhou, Z., Kong, B., Chao, Yu., Shi, X., Wang, M., Liu, W., Sun, Y., Zhang, Y., Yang, H., Yang, S., 2014. Tungsten oxide nanorods: an efficient nanoplatform for tumor CT imaging and photothermal therapy. *Sci. Rep.* 4, 3653.
- Zhou, X., Tian, Z., Kim, H.J., Wang, Y., Borui, Xu., Pan, R., Chang, Y.J., Di, Z., Zhou, P., Mei, Y., 2019. Rolling up MoSe<sub>2</sub> nanomembranes as a sensitive tubular photodetector. *Small* 15, 1902528.